Ultracompact, All-Passive Optical 90°-Hybrid on InP Using Self-Imaging

E. C. M. Pennings, R. J. Deri, R. Bhat, T. R. Hayes and N. C. Andreadakis

***Abstract*—Self-imaging in multimode waveguides has been used to realize a miniature (300 × 1750 μm^2), all-passive 90°-hybrid in GaInAsP/InP. We demonstrate excellent performance (splitting ratio of 97:99:104:99, low on-chip insertion losses ≤ 1 dB, only ±3° deviation from phase quadrature) and polarization-insensitive behavior at $\lambda_0 = 1.523$ µm. Experiments confirm simulations which predict that the splitting ratio and the IF phase relationships are much less sensitive to the coupler length than the insertion loss, thereby adding to the robustness of multimode interference devices.**

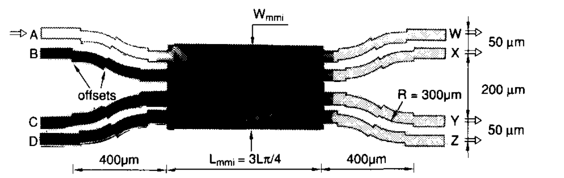

Fig. 1. Schematic layout of the optical 90°-hybrid and modal propagation analysis of the interference section.

OPTICAL hybrids provide a linear combination of two input fields at their outputs with a relative phase shift ϕ at one output [1]. Optical 90°-hybrids are crucial in phase-diversity homodyne receivers [2], in image rejection receivers [3], [4], in nonlinear Costas phase locked loops for PSK homodyne receivers [1], and are useful in avoiding the quadrature problem in interferometric sensors [5]. Previous schemes to realize an optical 90°-hybrid relied on specific states of polarization of the inputs [1], [6] or on optical phase shifters [7], [8]. These approaches result in wavelength- and polarization-dependent behavior. An alternative approach uses the self-imaging effect in multimode waveguides [9]. Using self-imaging, the entire 90°-hybrid can be realized as one single component as shown in Fig. 1, with the additional advantage that the phase quadrature condition is an inherent property of self-imaging. 90°-hybrids using self-imaging have been fabricated in glass using visible wavelengths and with ≈ 10 mm device lengths [5], [10]. Here, we report an InP-based integrated optical 90°-hybrid using self-imaging and operating at $\lambda_0 = 1.523$ μm. The device is ultracompact (submillimeter coupler length), which is essential for cost-effective monolithic integration with other optoelectronic devices, such as photodiodes [15].

Self-imaging [9] occurs in multimode waveguides of lengths $L = (p/q)3L_\pi \approx (p/q)4n_{\text{guide}}w_{\text{MMI}}^2/\lambda_0$, where L_π is the beat length between the fundamental and the first order mode and where n_{guide} and w_{MMI} are the refractive index and width of the multimode guide, respectively. The input is imaged into multiple output spots, of multiplicity determined by the integers p and q [9]. At $p/q = 1/4$, a four-fold image is formed, where each image contains one fourth of the input power as shown in Fig. 1. Simultaneous excitation of inputs A and C yields an IF beat signal at the four outputs that satisfy the phase quadrature relationship. This property is inherent to the four-fold self-image [5], [9], [10]. The location of the four images are symmetric with respect to the center and the quarter width points of the interference section. There is an interesting distinction between the 90°-hybrids reported in this letter and the recently reported 1 × 4 power splitters [12], that also employ broad multimode guides as the interference region. These power splitters differ in that they exhibit symmetric output phases, depend on symmetric excitation and consequently do not employ true self-images.

To optimize the hybrid, we performed numerical simulations employing a modal analysis based propagation model. Using 3.0 μm wide monomode waveguides and a 5.4 μm center-to-center guide separation, the interference section has a width of $w_{\text{MMI}} = 21.6$ μm which guides 13 TE modes and which has an optimum TE coupler length of 978 μm as shown in Fig. 2(a). Deviations from the optimum hybrid length of 978 μm cause comparable power decreases for all outputs (see Fig. 2(a) and [11]), unlike conventional power-conserving directional couplers. The simulated splitting ratio and relative phase relationship are used to calculate the image rejection ratio (IRR) and the electrical common mode rejection ratio $\text{CMRR}_{WZ} = -20 \log_{10} \{|i_W - i_Z|/(i_W + i_Z)\}$, with a similar definition for CMRR_{XY}. The IRR has been calculated by assuming identical photodetectors, by feeding the subtracted IF beat photocurrents $i_W - i_Z$ and $i_X - i_Y$ into a perfect microwave 3 dB (90°) hybrid and by taking the ratio of the electrical output powers. We con-

Manuscript received February 26, 1993.
E. C. M. Pennings was with Bellcore, Red Bank, NJ 07701. He is now with Philips Research Laboratories, 5600 JA Eindhoven, The Netherlands.
R. J. Deri was with Bellcore, Red Bank, NJ 07701. He is now with the Lawrence Livermore National Laboratory, L-220, Livermore, CA 94550.
R. Bhat and N. C. Andreadakis are with Bellcore, Red Bank, NJ 07701.
T. R. Hayes is with AT & T Bell Laboratories, Murray Hill, NJ 07974.
IEEE Log Number 9209448.

1041-1135/93$03.00

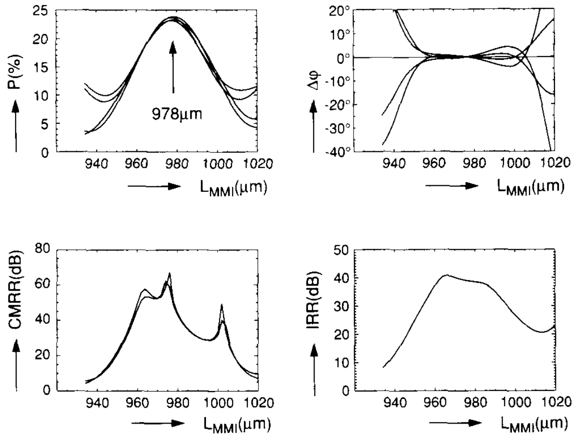

Fig. 2. Simulated TE performance. (a) relative output power, (b) phase deviation from the phase quadrature condition, (c) common mode rejection ratio and (d) image rejection ratio.

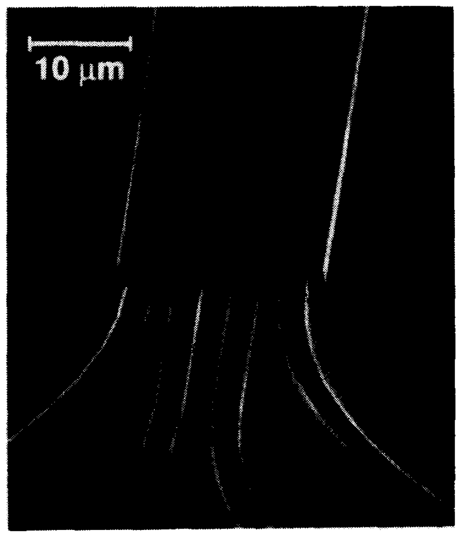

Fig. 3. Scanning electron micrograph showing the access region.

sider the IRR a good figure of merit since it involves all amplitude and phase information of the outputs. As a result of self-imaging, the CMRR and the IRR (Fig. 2(c) and (d), respectively) are much less sensitive to the hybrid length than the insertion loss. The 90°-hybrid is insensitive to polarization to the extent that the optimum coupler lengths are slightly different (978 μm for TE and 990 μm for TM polarization), but that this length difference is smaller than the length range of 28 μm where the loss penalty remains below 1 dB. The simulations also indicate that performance can be optimized by varying the location of the access guides and predict optimum performance for 5.1–5.7–5.1 μm center-to-center guide separations.

Optical 90°-hybrids were fabricated in an 1.6 μm-thick OMVPE grown GaInAsP layer ($\lambda_0 = 1.02$ μm) on InP (see also [11]) by means of conventional photolithography using methane/hydrogen (10% CH_4 in H_2) reactive ion etching. Etch depths of 2.2 to 2.5 μm were used to create monomode deeply etched waveguides. We employed radii of curvature of 300 μm [13], leading to a very short (400 μm) in- and output coupling network, and used lateral offsets of 0.15 μm or 0.35 μm as indicated in Fig. 1 to minimize the transition losses at junctions of straight and curved guides or junctions of oppositely curved guides, respectively. Fig. 3 shows an SEM micrograph of the completed device demonstrating smooth sidewalls for low scattering losses and well resolved gaps between the access guides. Straight guide losses as low as 1.4 dB/cm were measured using Fabry–Pérot techniques at $\lambda_0 =$ 1.523 μm after thinning and cleaving. This value is among the lowest for deeply-etched waveguides. For coupler characterization an SiO_x antireflection coating ($r \leq 0.5 \times 10^{-3}$) was applied.

Three hybrids on the same chip with coupler lengths L_{MMI} of 935, 945, and 955 μm were completely characterized (see Fig. 5). Performing transmission measurements with respect to straight reference guides, low on-chip insertion losses were measured (≤ 1 dB). The values include imperfect self-images in the interference section as well as propagation and bending losses in the access network. By comparing the measured optimum TE coupler length of 935 μm and the predicted value of 978 μm, a deviation from the design feature size of -0.4 μm can be deduced. Splitting ratios were determined by measuring the transmitted power for all combinations of inputs and outputs. A best splitting ratio was found of $W{:}X{:}Y{:}Z$ = 97:99:104:99 corresponding to a best CMRR of 32 and 40 dB for the inner two and the outer two ports, respectively. A worst value for the CMRR of 20 dB was found for three devices and both polarizations. Observed performance was slightly better for TM than for TE polarization. Optimum TE and TM performances are achieved for slightly different hybrid lengths (as predicted), but the 945 μm hybrid can be used for polarization-independent applications while introducing a small performance degradation. The phase relationships of the IF signal have been measured with a self-heterodyne technique [14]. Light from a $\lambda_0 = 1.523$ μm He–Ne laser was split in two by a 3 dB fiber coupler. The light in one of the arms was shifted in frequency by approximately 100 Hz by means of a phase shifter consisting of a fiber coiled around a piezoelectric drum, to which a sawtooth voltage of $V_{2\pi} =$ 19 V is applied. Precautions were taken in order to reduce phase fluctuations in both arms due to temperature differences. Fig. 4 shows that the IF beat signal satisfies the phase quadrature condition. The device with best splitting ratio (955 μm and TM pol.) also shows the best values for the IF phase differences: $42°/135°/-42°/-133°$ for $W/X/Y/Z$ outputs which corresponds to IRR = 31 dB. The deviation from the ideal phase quadrature condition is smaller than $\pm 3°$ (or 6° between any two outputs) for this hybrid. As shown in Fig. 5, phase deviations from the ideal quadrature condition were smaller than $\pm 8°$ for all three devices and for both polarizations.

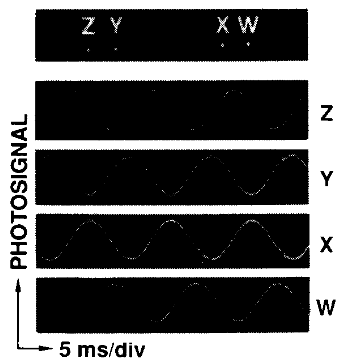

Fig. 4. Near field view of the output facet (top) and oscilloscope trace of the measured IF beat signal at the four outputs (bottom).

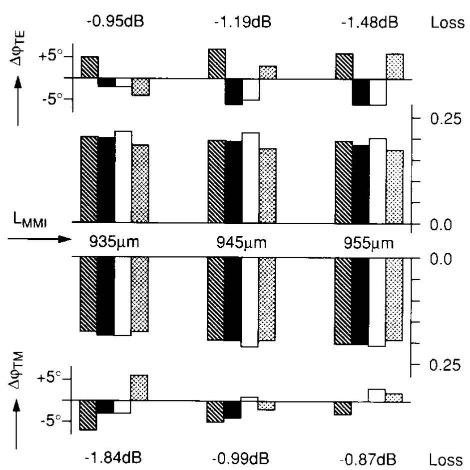

Fig. 5. Measured performance of three 90°-hybrids. Bars are for W/X/Y/Z outputs, respectively.

In conclusion, we have reported on an InP-based integrated all-passive optical 90°-hybrid using self-imaging. The robustness of the self-imaging effect makes tuning superfluous and leads to an ultracompact device consisting of one single interference section. The performance is insensitive to polarization, so that the devices can be used for polarization independent applications, such as polarization diversity receivers. In addition, we have shown previously that devices based on self-imaging are fairly insensitive to wavelength and temperature [11]. These devices do, however, require careful control of the coupler-width; our calculations show that a feature-size deviation of 0.2 μm leads to a loss increase of 2 dB. Practical designs can anticipate a potential penalty by using a small number ($\approx$ 5) of different coupler lengths. With regard to applications, we envision that by combining this hybrid with ultracompact polarization diversity photodetectors [15] an ultra-compact phase-diversity or image-rejection polarization-diversity coherent receiver chip can be fabricated.

Acknowledgment

The authors gratefully acknowledge discussions with and help from L. B. Soldano, R. Welter, D. A. Smith, A. Scherer, L. F. Tiemeijer, and L. M. Schiavone.

References

[1] W. R. Leeb, "Optical 90°-hybrid for costas-type receivers," *Electron. Lett.*, vol. 26, no. 18, pp. 1431–1432, 1990.

[2] L. G. Kazovsky, R. Welter, A. F. Elrefaie, and W. Sessa, "Wide-linewidth phase diversity homodyne receivers," *J. Lightwave Technol.*, vol. 6, pp. 1527–1536, Oct. 1988.

[3] B. S. Glance, "An optical heterodyne mixer providing image-frequency rejection," *J. Lightwave Technol.*, vol. LT-4, pp. 1722–1725, Nov. 1986.

[4] G. Ishikawa, T. Naito, Y. Yorita, H. Nakamoto, and T. Chikama, "High noise immunity of CP-FSK with an optical heterodyne image-rejection receiver in optical-amplifier repeated systems," in *Proc. ECOC'92*, Berlin, Germany, 1992, pp. 365–368.

[5] Th. Niemeier and R. Ulrich, "Quadrature outputs from fiber interferometer with 4 × 4 coupler," *Opt. Lett.*, vol. 11, no. 10, pp. 677–679, 1986.

[6] W. R. Leeb, "Realization of 90°- and 180° hybrids for optical frequencies," *Arch. Elek. Übertragung*, vol. 37, no. 5/6, pp. 203–206, 1983.

[7] D. Hoffmann, H. Heidrich, G. Wenke, R. Langenhorst, and E. Dietrich, "Integrated optics eight-port 90° hybrid on $LiNbO_3$," *J. Lightwave Technol.*, vol. 7, no. 5, pp. 794–798, 1989.

[8] L. B. Soldano *et al.*, "New all-passive 4 × 4 planar phase diversity network," in *Proc. ECOC-IOOC'91*, Paris, France, post-deadline papers 1991, pp. 96–99.

[9] R. Ulrich and G. Ankele, "Self-imaging in homogeneous planar optical waveguides," *Appl. Phys. Lett.*, vol. 27, no. 6, pp. 337–339, 1975.

[10] P. Roth, "Passive integrated optic mixer providing quadrature outputs," in *Proc. 5th ECIO'89*, SPIE, vol. 1141, pp. 169–173, 1989.

[11] E. C. M. Pennings, R. J. Deri, A. Scherer, R. Bhat, T. R. Hayes, N. C. Andreadakis, M. K. Smit, L. B. Soldano, and R. J. Hawkins, "Ultracompact, low-loss directional couplers on InP based on self-imaging by multimode interference," *Appl. Phys. Lett.*, vol. 59, no. 16, pp. 1926–1928, 1991.

[12] J. M. Heaton, R. M. Jenkins, D. R. Wright, J. T. Parker, J. C. H. Birbeck, and K. P. Hilton, "Novel 1-to-N way integrated optical beam splitters using symmetric mode mixing in GaAs/AlGaAs multimode waveguides," *Appl. Phys. Lett.*, vol. 61, no. 15, pp. 1754–1756, 1992.

[13] E. C. M. Pennings, R. J. Deri, and R. J. Hawkins, "Simple method for estimating usable bend radii of deeply etched optical rib waveguides," *Electron. Lett.*, vol. 27, no. 17, pp. 1532–1534, 1991.

[14] D. A. Smith, J. E. Baran, J. L. Jackel, R. E. Wagner, and R. Welter, "Mode-evolution-type optical beam combiner for coherent receivers," in *Proc. IPRC'91*, Monterey, CA, 1991, p. 80.

[15] R. J. Deri, E. C. M. Pennings, A. Scherer, A. S. Gozdz, C. Caneau, N. C. Andreadakis, V. Shah, L. Curtis, R. J. Hawkins, J. B. D. Soole, and J.-I. Song, "Ultracompact monolithic integration of balanced, polarization diversity photodetectors for coherent lightwave receivers," *IEEE Photon. Technol. Lett.*, vol. 4, pp. 1238–1240, Nov. 1992.